Bidirectional Elongation Strategy Using Ambiphilic Radical Linchpin for Modular Access to 1,4-Dicarbonyls via Sequential Photocatalysis

Akira Matsumoto,*,† Natsumi Maeda,† and Keiji Maruoka*,†,‡

†Graduate School of Pharmaceutical Sciences, Kyoto University, Sakyo, Kyoto 606-8501, Japan

‡School of Chemical Engineering and Light Industry, Guangdong University of Technology, Guangzhou 510006, China

KEYWORDS: photoredox catalysis • sequential photocatalysis • phosphonium ylides • ambiphilic linchpin

ABSTRACT: Organic molecules which connect themselves with multiple substrates by sequential C–C bond formations can be utilized as linchpin compounds in multicomponent process. While they are useful for rapidly increasing the molecular complexity, most of the reported linchpin coupling methods rely on the use of organometallic species as strong carbon nucleophiles to form C–C bonds, which narrows the functional group compatibility. Here, we describe a metal-free, radical-mediated coupling approach using a formyl-stabilized phosphonium ylide as a multifunctional linchpin under visible-light photoredox conditions. The present method demonstrates an ambiphilic character of the phosphonium ylide, which serves both as a nucleophilic and an electrophilic carbon-centered radical source. The stepwise and controllable generation of these radical intermediates allows sequential photocatalysis involving two mechanistically distinct radical additions, both of which are initiated by the same photocatalyst in one pot with a high functional-group tolerance. The methodology enables a bidirectional assembly of the linchpin with two electronically differentiated alkene fragments and thus offers a rapid and modular access to 1,4-dicarbonyl compounds as versatile synthetic intermediates.

INTRODUCTION

Rapid assembly of widely available substrates into synthetically valuable products is of prime importance in modern organic chemistry.[1] The use of small organic molecules which connect themselves with multiple substrates by a sequential C–C bond-forming process has offered a bidirectional approach to increase the molecular complexity with a high modularity (Figure 1a).[2] Such multicomponent protocols utilizing linchpin compounds have enabled the expeditious construction of complex building blocks for natural products and biologically important molecules.[3] However, their C–C bond-forming processes rely heavily on the use of organometallic reagents as strong nucleophiles, which narrows the scope of accessible products due to the limited functional group compatibility. Moreover, complicated manipulations (i.e., cryogenic conditions with strict prohibition of water) are frequently required to control the reactivity of these reagents and intermediates. On the other hand, the chemistry of radical species can provide a complementary approach to that of ionic species for new bond disconnections.[4] The recent advances of methodologies for the generation of radical species, such as photoredox catalysis[5] and electrocatalysis,[6] has made these conditions milder and more practical. Despite these breakthroughs, the linchpin coupling strategy based on radical-mediated C–C bond formations has been less explored.[7]

Aliphatic aldehydes are one of the simplest linchpin motifs with ambiphilic character: while the formyl carbon is electrophilic, the α-carbon center can be a nucleophile via an enolate or enamine intermediate (Figure 1b). To date, several classic transformations associated with carbonyl groups, such as aldol reaction, Mannich reaction, and Wittig olefination, have been applied as a method for C–C bond formation with aldehyde linchpin.[8] Similarly, in the field of radical chemistry, two different carbon-centered radicals can be generated from aldehydes. For example, hydrogen-atom transfer (HAT) from the formyl C–H bond affords acyl radicals as a nucleophilic radical.[9,10] On the other hand, the single-electron transfer (SET) of various carbonyl compounds and their derivatives generates electrophilic radicals at the α-carbon of carbonyl group.[11,12] Based on these backgrounds, we envisioned that the controlled activation of a specific aldehyde unleashes its latent reactivity both as a nucleophilic and an electrophilic carbon-centered radical in a sequential manner, thus functioning as an ambiphilic radical linchpin. Here, we report the realization of this concept by using (triphenylphosphoranylidene)acetaldehyde (**P1**) as a commercially available aldehyde to initiate two mechanistically distinct radical processes (Figure 1c). With a single photoredox catalyst (PC), a one-pot sequence involving two different radical addition reactions via the formation of intermediate ylide **P2** is established by a stepwise and controllable generation of nucleophilic and electrophilic carbon-centered radicals. This approach allows a modular access to 1,4-dicarbonyls, which are versatile synthetic intermediates and ubiquitous motifs found in natural products,[13] from two electronically differentiated alkene fragments. The mild and practical conditions of visible-light photoredox catalysis enable a rapid assembly of complex molecules with various functional groups which are difficult to apply to the polar linchpin coupling strategy.

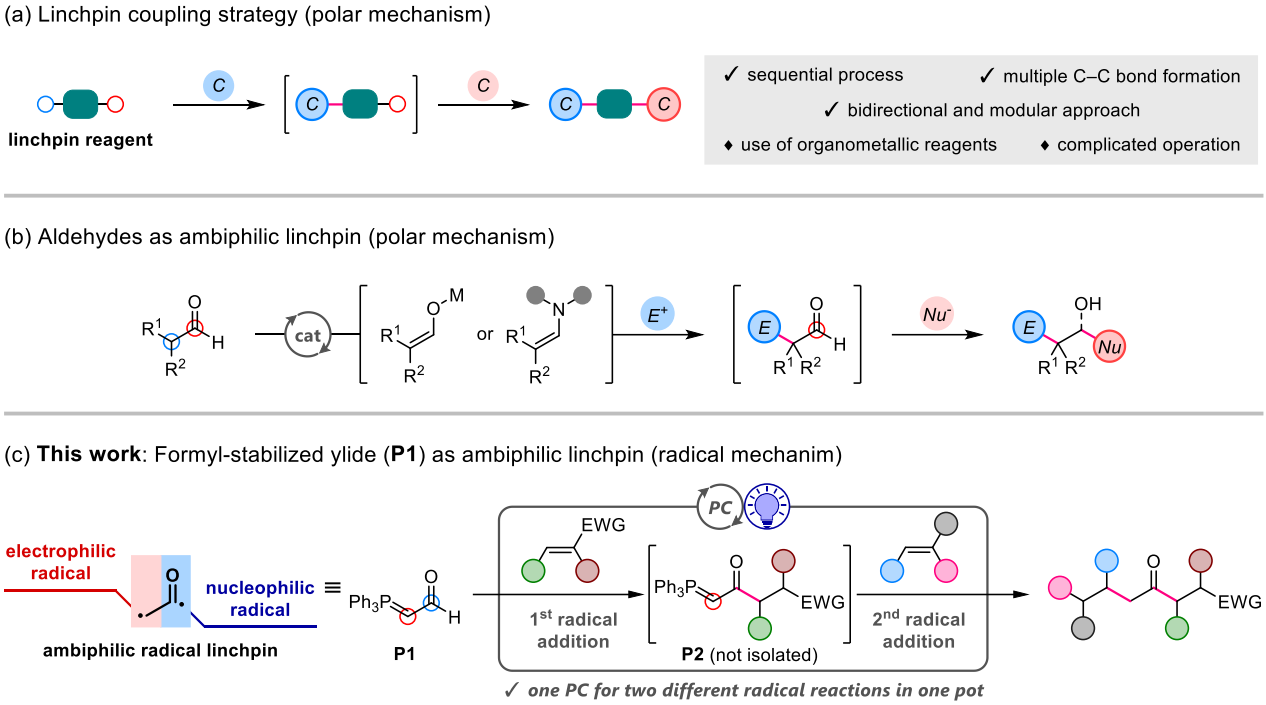

Figure 1. (a) General scheme for linchpin coupling strategy. (b) Aliphatic aldehydes as ambiphilic linchpin. (c) Sequential photocatalysis using formyl-stabilized phosphonium ylide (**P1**) as ambiphilic radical linchpin. EWG = electron-withdrawing group.

RESULTS AND DISCUSSION

Optimization of Reaction Conditions. We commenced our study with the investigation of the reactivity of **P1** as a precursor of nucleophilic acyl radical. Initially, it was expected that the desired acyl radical would be generated via photoinduced HAT catalysis.[10,14] To our surprise, a brief survey of the conditions revealed that the reaction of **P1** and benzyl acrylate (**1a**) afforded the desired product **P2a** *in the absence of any HAT catalyst*. Further screening of photocatalysts led us to find 4CzIPN as the optimal catalyst (Table 1, entry 1. See the Supporting Information (SI) for details). Other catalysts with similar redox properties to 4CzIPN, such as 3CzClIPN and {[Ir[dF(CF$_3$)ppy]$_2$(dtbbpy)}PF$_6$ ([Ir]-2), also afforded high yields of **P2a**, while strongly reducing catalyst (*fac*-Ir(ppy)$_3$: [Ir]-1) or oxidizing catalyst (Me-Acr$^+$) were not effective (Table 1, entries 2–5). The use of other solvents, including DMSO, CH_2Cl_2, and acetone, showed lower efficiency than MeCN (Table 1, entries 6–8). Several control experiments and radical-trapping experiments by TEMPO (2,2,6,6-tetramethylpiperidine-1-oxyl) suggested a radical mechanism via excitation of the photocatalyst induced by visible light (Table 1, entries 9–10). We then investigated the scope of Michael acceptors. Although the purification of the obtained ylides **P2** were found to be difficult, a wide range of acceptors including α,β-unsaturated esters, ketones, sulfone, and phosphonate successfully converted to the corresponding products **P2** generally in high yields according to the crude ^{1}H NMR analysis (See SI for the full list of acceptor scope).

Table 1: Optimization of Reaction Conditions for 1st Step.

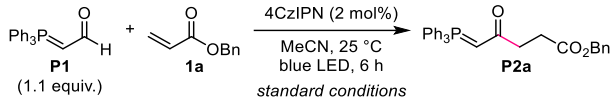

entry	deviation from standard conditions	**P2a** (%)[a]
1	none	92
2	3CzClIPN instead of 4CzIPN	88
3	[Ir]-1 instead of 4CzIPN	9
4	[Ir]-2 instead of 4CzIPN	92
5	Me-Acr$^+$ instead of 4CzIPN	N.D.
6	DMSO instead of MeCN	49
7	CH_2Cl_2 instead of MeCN	55
8	acetone instead of MeCN	86
9	without photocatalyst or light	N.D.
10	with TEMPO (2.0 equiv.)	N.D.

[a] Yields were determined by ^{1}H NMR using 1,1,2,2-tetrachloroethane as an internal standard. N.D. = Not Detected.

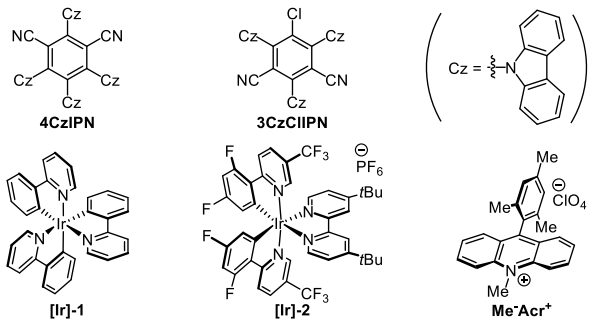

Next, we turned our attention to the 2nd step, where an electrophilic carbon-centered radical is generated from ylide **P2** to react with unactivated alkene fragments.[11] Recently, Miura and Murakami have reported a convenient method for the generation of (alkoxycarbonyl)methyl radical from ester-stabilized phosphonium ylides based on photoredox catalysis.[15] They used ascorbic acid with these ylides to form the corresponding phosphonium salts, which are subsequently reduced by highly reducing photoredox catalyst [Ir]-1 (Figure 2a). However, our initial attempt to generate an electrophilic radical from acyl-stabilized ylide **P2'** under the identical conditions was unsuccessful and the reaction with 4-phenyl-1-butene (**2a**) afforded the desired ketone product **3a** in a significantly low yield (7 % NMR yield). Moreover, while a highly reducing photocatalyst would be favorable for this method as the 2nd step, a more oxidizing photocatalyst such as 4CzIPN is rather required at the 1st step. Such a discrepancy of the required potential of photoredox catalysts between each step would be problematic for the realization of one-pot sequential process. Therefore, we sought to develop alternative conditions where the same photocatalyst can promote both the 1st and 2nd steps. Specifically, we focused on a method utilizing carbon dioxide radical anion ($CO_2^{\bullet-}$) as a potent single-electron reductant ($E_{1/2}$ = −2.2 V vs saturated calomel electrode, SCE),[16] which would smoothly reduce a phosphonium salt derived from **P2** to generate the desired electrophilic radical. Given that $CO_2^{\bullet-}$ can be generated from metal formate under photochemical conditions,[17] we envisioned that $CO_2^{\bullet-}$ can be generated from a formate anion or its equivalent as a counteranion of phosphonium salt, which is formed in situ from the corresponding Brønsted acid with ylide **P2** (Figure 2b).

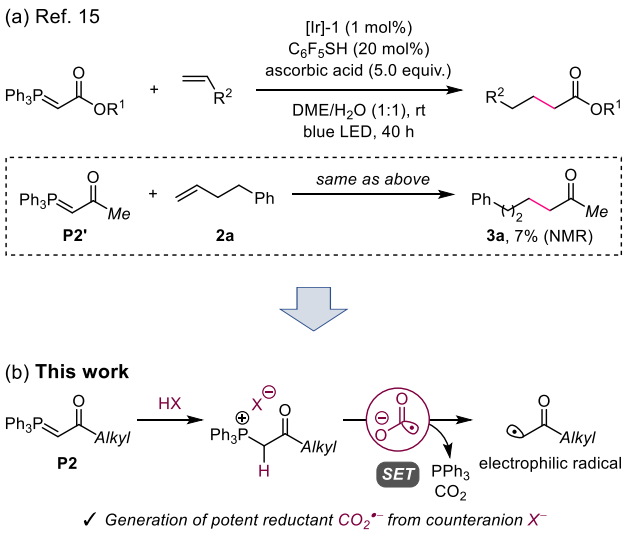

Figure 2. Strategy for the generation of electrophilic radical from phosphonium ylide at the 2nd step.

Based on our hypothesis, the effect of acids was investigated for the reaction of ylide **P2'** with **2a** in the presence of 4CzIPN and methyl thiosalicylate (**S1**) as a thiol HAT catalyst under irradiation of blue light-emitting diode (LED, λ_{max} = 448 nm) (Table 2). While the addition of conventional Brønsted acids (Table 2, entries 1–3) or ascorbic acid (Table 2, entry 4) were found to be less effective, the use of formic acid remarkably improved the yield of **3a** (Table 2, entry 5), which is consistent with our proposed mechanism (Figure 2b). A further exploration of Brønsted acids acting as a precursor of $CO_2^{\bullet-}$ revealed that oxalic acid dihydrate ($(CO_2H)_2{\cdot}2H_2O$) afforded **3a** in a better yield (Table 2, entry 6). A screening of other parameters identified cosolvent of DMSO and H_2O (v/v = 9/1) as a suitable solvent (Table 2, entry 7). The replacement of 4CzIPN with [Ir-2], another suitable photocatalyst for the 1st step, was found to be ineffective for the 2nd step (Table 2, entry 8). The prolonged reaction time provided **3a** in a sufficiently high yield (Table 2, entry 9). Control experiments established the necessity of photocatalyst and light irradiation (Table 2, entry 10).

Table 2: Optimization of Reaction Conditions for 2nd Step.

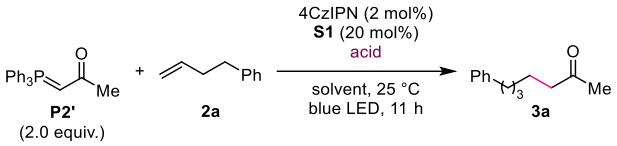

entry	acid (equiv.)	solvent	**3a** (%)[a]
1	CF_3CO_2H (2.0)	DMSO	19
2	HBF_4 (2.0)	DMSO	7
3	TsOH (2.0)	DMSO	4
4	ascorbic acid (5.0)	DMSO	N.D.
5	HCO_2H (5.0)	DMSO	54
6	$(CO_2H)_2{\cdot}2H_2O$ (2.0)	DMSO	67
7	$(CO_2H)_2{\cdot}2H_2O$ (2.0)	DMSO/H_2O (9/1)	74
8[b]	$(CO_2H)_2{\cdot}2H_2O$ (2.0)	DMSO/H_2O (9/1)	21
9[c]	*$(CO_2H)_2{\cdot}2H_2O$ (2.0)*	*DMSO/H_2O (9/1)*	*86 (84)*
10[c,d]	$(CO_2H)_2{\cdot}2H_2O$ (2.0)	DMSO/H_2O (9/1)	trace

[a] Yields were determined by ^{1}H NMR using 1,1,2,2-tetrachloroethane as an internal standard. The isolated yield is shown in parentheses. [b] [Ir-2] was used instead of 4CzIPN. [c] Reaction time was 20 h. [d] No light or photocatalyst.

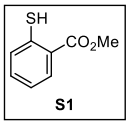

Mechanistic Investigations. To better understand the reaction mechanism, a series of analytical and experimental studies for the 1st and 2nd steps were respectively carried out (Figure 3, see SI for details). Stern–Volmer fluorescence quenching studies for the 1st step revealed that only **P1** quenches the excited state of 4CzIPN and acceptor **1a** does not (Figure 3, 1-A). In addition, electrochemical analysis of **P1** indicated its oxidation potential as 0.96 V vs SCE) (Figure 3, 1-B), which is lower than the reduction potential of the excited state of 4CzIPN ($E(PC^*/PC^{\bullet-})$ = 1.35 V vs SCE).[18] Hence, the reaction proceeds with the single-electron oxidation of phosphonium ylide via a reductive quenching cycle to generate a new radical species **I** (Figure 3, 1-C). At this point, we reasoned that two electron-withdrawing groups of **I**, a carbonyl moiety and a quaternary phosphonium moiety, would render the neighboring carbon radical center highly electrophilic, which can act as a HAT mediator to abstract a hydrogen atom from the formyl C–H bond of **P1** to

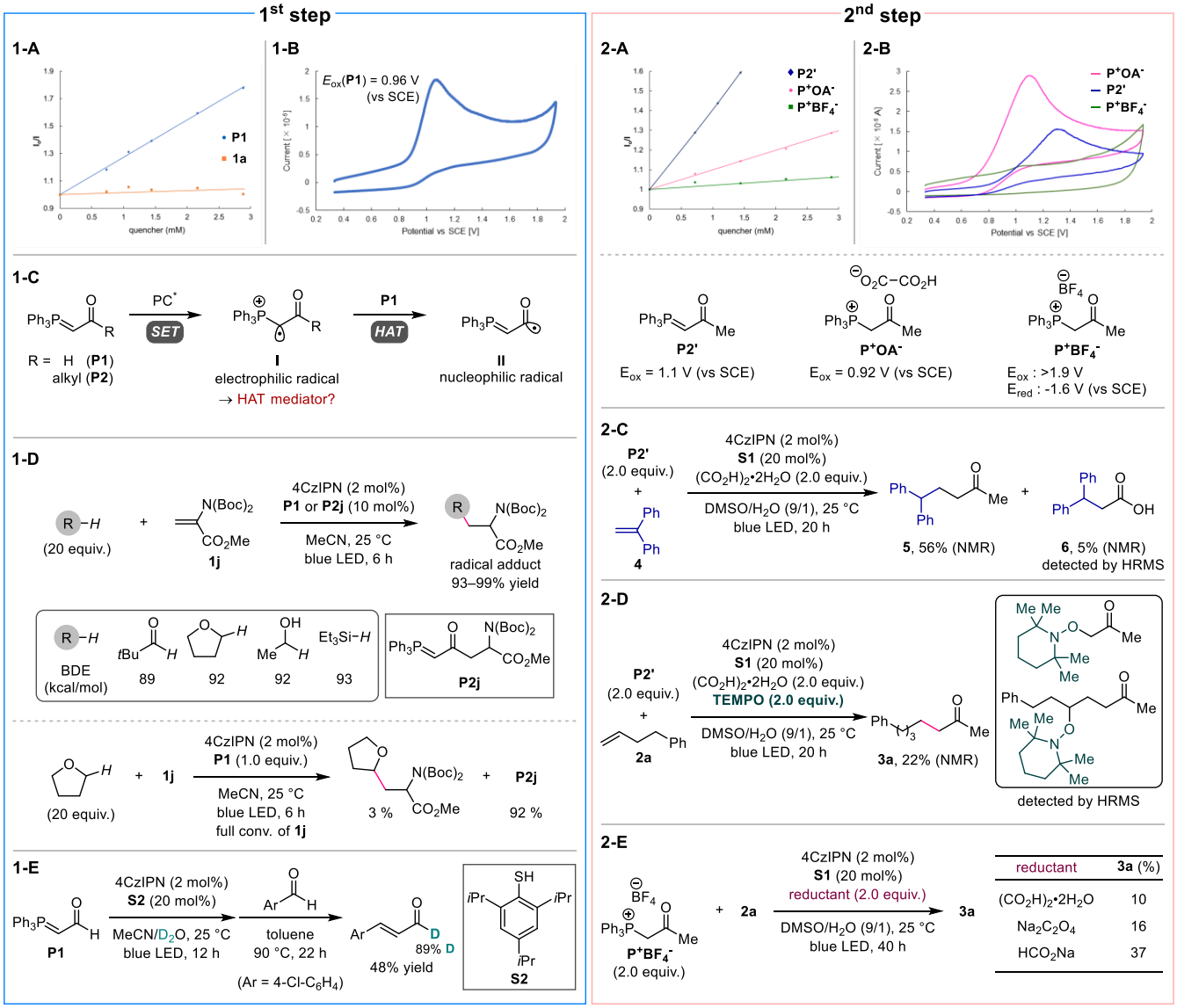

Figure 3. Mechanistic investigations for the 1st step (left) and the 2nd step (right). (1-A) Stern–Volmer quenching studies for the 1st step. (1-B) Cyclic voltammogram of **P1**. (1-C) Possible mechanism for generation of acyl radical **II**. (1-D) Evaluation of HAT ability of phosphonium ylides. (1-E) H/D exchange of **P1**. (2-A) Stern–Volmer quenching studies for the 2nd step. (2-B) Comparison of redox potential of phosphonium species. (2-C) Radical-trapping experiment with **4**. (2-D) Radical-trapping experiment with TEMPO. (2-E) Importance of ion-pair formation.

generate the nucleophilic acyl radical **II**.[10] To provide more evidence for the generation of electrophilic radical **I**, the HAT ability of phosphonium ylides was investigated in the photoinduced alkylation of C–H or Si–H bonds using Michael acceptor **1j** (Figure 3, 1-D).[19] Indeed, the use of a catalytic amount of phosphonium ylide **P1** or **P2j**, both of which are included in the reaction system of the 1st step, was found to be effective to promote the reactions of several substrates bearing C–H or Si–H bonds with those bond-dissociation energies (BDEs) ranging from 89–93 kcal/mol, affording the corresponding radical adducts in significantly high yields in all cases. Moreover, the use of a stoichiometric amount of **P1** in the reaction of **1j** and a large excess amount of THF dominantly produced **P2j** with a detection of a small amount of a THF-derived radical adduct, indicating the fast conversion of **P1** to **P2j** before starting the reaction with THF. These results are consistent with the formation of electrophilic radical **I** serving as a HAT mediator in the 1st step of our method. While the HAT ability of the electrophilic radical derived from **P1** is still unclear, the one derived from product ylide **P2** can abstract a formyl C–H bond and is likely to be involved in the productive photocatalytic cycle of acyl radical **II**. Regarding the evidence for the generation of acyl radical **II**, **P1** was subjected to the conditions for photocatalytic deuteration of formyl C–H bonds mediated by thiol catalyst, which can donate a deuterium atom to nucleophilic acyl radicals (Figure 3, 1-E).[20] As expected, the reaction of **P1** in the presence of 4CzIPN and **S2** as the thiol catalyst in cosolvent of MeCN and D_2O, followed by the Wittig reaction with 4-chlorobenzaldehyde, afforded deuterated 4-chlorocinnamaldehyde with a high deuterium incorporation at the formyl group. This result supports the generation of acyl radical from **P1**.

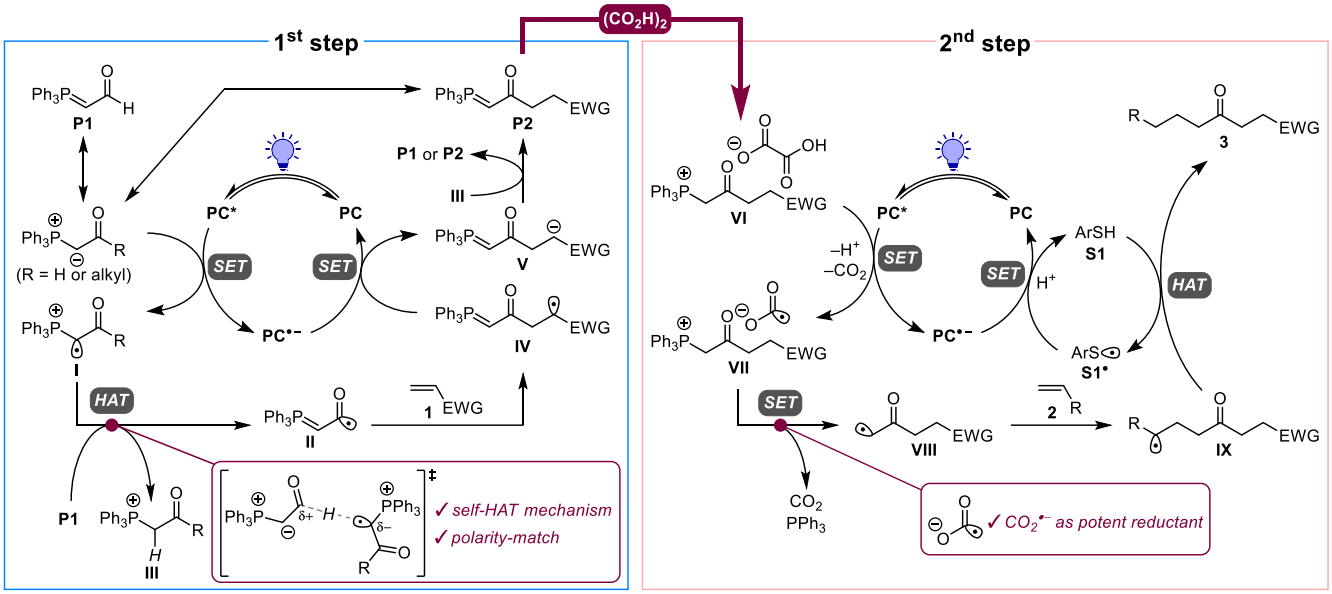

Figure 4. Proposed mechanism for sequential photocatalysis.

Next, to identify an actual radical precursor responsible for the 2nd step, Stern–Volmer fluorescence quenching studies and electrochemical analysis of ylide **P2'** and the corresponding phosphonium salts were carried out (Figure 3, 2-A and 2-B). The Stern–Volmer plots showed that the quenching rate of phosphonium oxalate (**P⁺OA⁻**), which was prepared by mixing an equimolar amount of **P2'** with oxalic acid, is different from those of **P2'** and phosphonium tetrafluoroborate (**P⁺BF₄⁻**). Notably, **P⁺OA⁻** quenches the excited state of 4CzIPN whereas **P⁺BF₄⁻** hardly quenches it, indicating the non-innocent role of the counteranion of **P⁺OA⁻**. The cyclic voltammetry reflected different redox behaviors of these species (Figure 3, 2-B). While **P2'** and **P⁺OA⁻** indicated the oxidation potential at 1.1 V vs SCE and 0.92 V vs SCE, respectively, **P⁺BF₄⁻** did not show any obvious oxidation peak within the measurement range. Instead, the reduction potential of **P⁺BF₄⁻** was found to be −1.6 V vs SCE. Given the redox potential of 4CzIPN (E(PC*/PC•⁻) = 1.35 V vs SCE; E(PC/PC•⁻) = −1.21 V vs SCE),[18] these observations well explain the experimental results: the use of conventional acid such as HBF_4 led to a low yield of **3a** due to a less efficient SET between 4CzIPN and the corresponding phosphonium salt **P⁺BF₄⁻** (Table 2, entry 2). However, the use of $(CO_2H)_2{\cdot}2H_2O$ was effective because the resulting phosphonium oxalate **P⁺OA⁻** can be oxidized by 4CzIPN, probably followed by the degradation of the oxalate anion to generate potent reductant $CO_2^{\bullet-}$ (Table 2, entry 6).[21] Thus, we next sought to obtain the evidence for generation of $CO_2^{\bullet-}$ by capturing it with 1,1-diphenylethylene (**4**) as a radical-trapping agent (Figure 3, 2-C). Indeed, after a reaction of **P2'** with **4** under optimal conditions, the expected radical adduct **6** could be detected by ^{1}H NMR analysis and high-resolution mass spectrometry (HRMS) along with **5** as the major product. Furthermore, another radical-trapping experiment using TEMPO suppressed the formation of ketone product **3a** and two kinds of TEMPO adducts were detected by HRMS, indicating the generation of acetyl-substituted carbon radical and the subsequent radical addition to alkene **2a** (Figure 3, 2-D). Lastly, to confirm the effect of the formation of an ion pair between a phosphonium and an oxalate, phosphonium salt **P⁺BF₄⁻** was subjected to conditions for the 2nd step using several $CO_2^{\bullet-}$ precursors (Figure 3, 2-E). None of the examined reductants including oxalic acid, oxalate salt, and formate salt showed comparable results to the optimized conditions, indicating that the smooth formation of the ion pair via acid-base reaction between phosphonium ylide **P2'** and oxalic acid contributes to the efficient single-electron reduction of the phosphonium salt.

Taken together, we propose a mechanism for the whole process of our method as shown in Figure 4. For the 1st step, the single-electron oxidation of ylide **P1** (or **P2** after the first catalytic cycle) by the excited state of 4CzIPN (**PC***) generates highly electrophilic radical **I**, which can act as a HAT mediator as demonstrated in 1-D of Figure 3. Here, the negative charge at α-carbon of **P1** renders its formyl C–H bond highly hydridic. Therefore, the HAT between **I** and **P1** would take place selectively due to the polarity-matching effect[22] and acyl radical **II** is efficiently generated along with phosphonium salt **III**. Since **II** has a nucleophilic character, it undergoes Giese-type addition to Michael acceptor **1** to afford intermediate **IV**. The subsequent SET by the reduced form of photocatalyst (**PC•⁻**) converts **IV** to **V**, which deprotonates a moderately acidic α-C–H bond of **III** to furnish the intermediate ylide **P2**. After **P1** is completely converted to **P2** at the 1st step, oxalic acid is added to the system to form phosphonium oxalate **VI**, which is then engaged in the catalytic cycle of the 2nd step. As discussed in 2-A and 2-B of Figure 3, **VI** can be oxidized by the same photocatalyst of the 1st step. Upon the following deprotonation and decarboxylation, $CO_2^{\bullet-}$ is generated as a potent reductant, which facilitates the cleavage of a C–P bond in the phosphonium moiety of the same ion pair **VII** to yield electrophilic radical **VIII**. The addition of **VIII** to unactivated alkene **2** provides intermediate **IX**, which accepts a hydrogen atom from thiol catalyst **S1** to afford the desired product **3**. Finally, the resulting thiyl radical **S1•** is reduced by **PC•⁻** with the concurrent protonation, closing the catalytic cycle. We observed quantum yield (Φ) values much lower than 1 for both steps (Φ = 6.3 ×

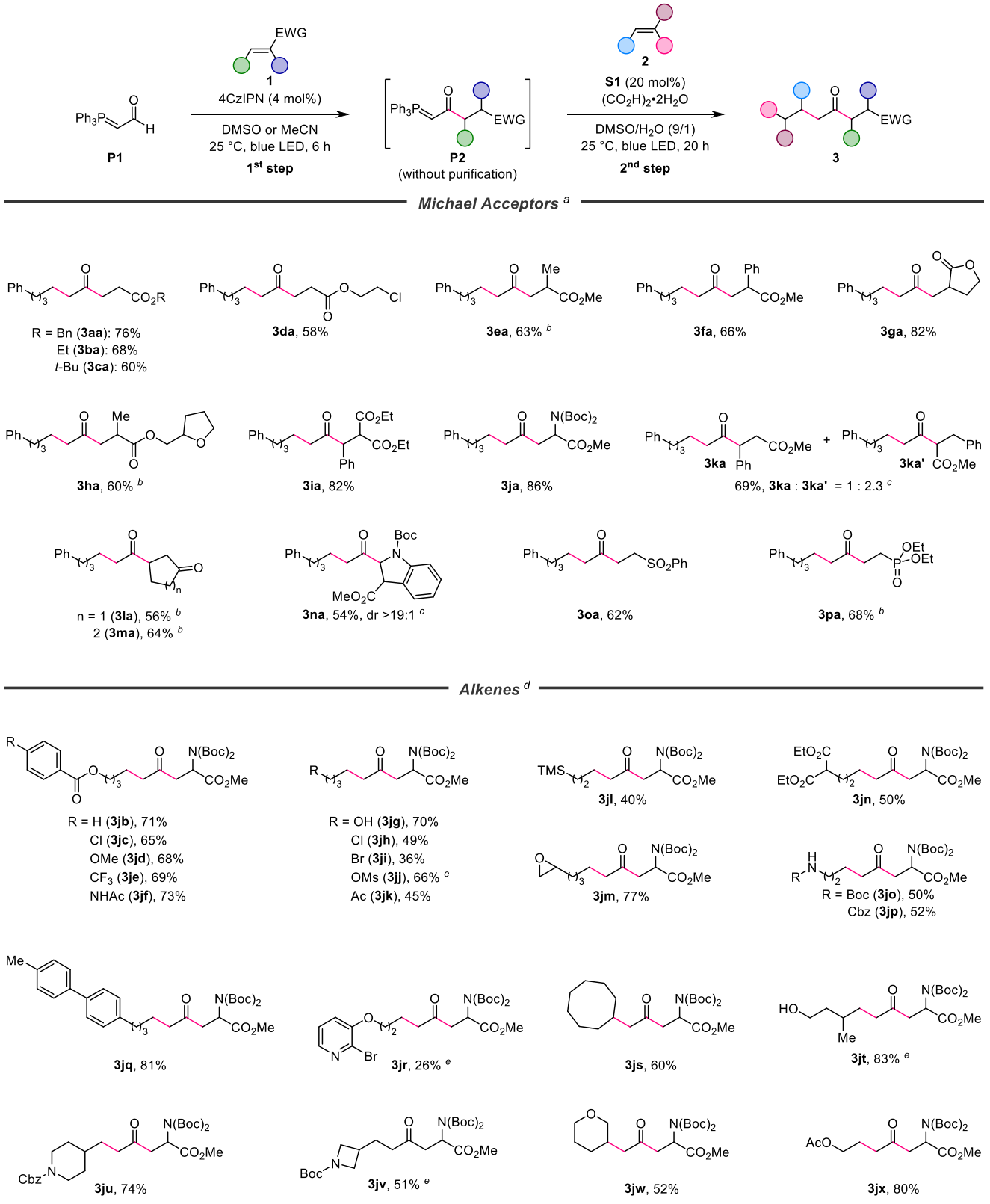

Figure 5. Substrate Scope for sequential photocatalysis. Reaction conditions: [1st step] **P1** (0.44 mmol), **1** (0.40 mmol), and 4CzIPN (0.0080 mmol) in MeCN or DMSO, blue LED (λ_{max} = 448 nm), 25 °C, 6 h; [2nd step] **P2** (not isolated), **2** (0.20 mmol), $(CO_2H)_2 \cdot 2H_2O$ (0.40 mmol), and methyl thiosalicylate (**S1**, 0.040 mmol) in DMSO/H_2O (9/1), blue LED (λ_{max} = 448 nm), 25 °C, 20 h. Isolated yields over 2 steps are shown. See SI for full experimental details. [a] MeCN (4.0 mL) was used as a solvent for the 1st step. [b] $LiBF_4$ (0.080 mmol) was added for the 1st step. [c] Regioisomeric ratio and diastereomer ratio (dr) were determined by ^1H NMR of the crude product. [d] DMSO (2.0 mL) was used as a solvent for the 1st step. [e] Reaction time for the 2nd step was 40 h.

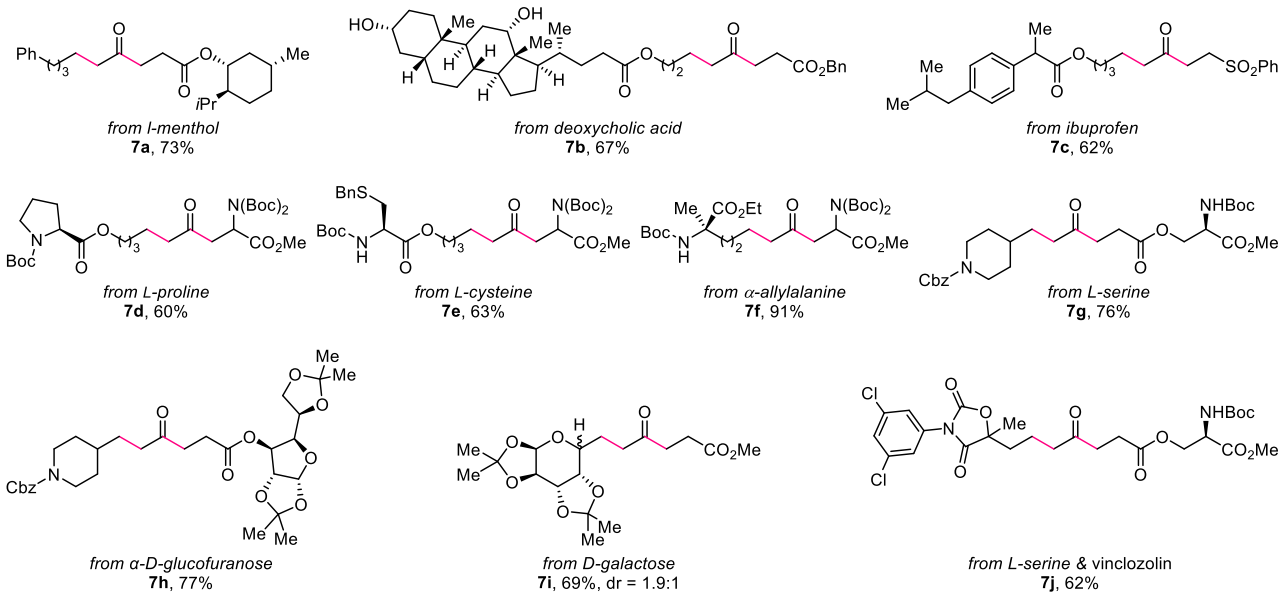

Figure 6. Radical linchpin coupling with biorelevant molecules. See SI for full experimental details.

10^{-2} for the 1st step and 3.0×10^{-3} for the 2nd step. See SI for details), which are consistent with closed catalytic cycles and thus the mechanism of sequential photocatalysis.

Development of Sequential Process. Based on the optimized conditions for each step together with the proposed mechanism, we sought to develop a one-pot protocol for sequential photocatalysis using ambiphilic radical linchpin **P1** with two alkene fragments (**1** and **2**) to access unsymmetrical ketone product **3** (Figure 5). Gratifyingly, reaction conditions established for each step were successfully combined to realize the sequential process, and intermediate ylide **P2** formed after the 1st step could be directly used for the 2nd step without purification (see SI for detailed protocols). Of note, the photocatalyst added before the 1st step was still active at the 2nd step, establishing a unique protocol for the sequential process where a single photocatalyst promotes two mechanistically distinct radical reactions successively in one pot. With the optimized experimental protocols in hand, we sought to evaluate the scope of the sequential photocatalysis. Firstly, a variety of Michael acceptors **1** were employed for the 1st step of our method to unite them with **P1** and **2a**, affording 1,4-dicarbonyl compounds in most cases. Acrylate derivatives were well tolerated to give the desired γ-oxoesters **3aa**–**3ka** in moderate to good yields. In the case of acceptors with insufficient reactivity at the 1st step, the addition of $LiBF_4$ was found to be effective, providing acceptable yields of the products. Highly activated alkenes furnished the corresponding products **3ia**–**3ja** in high yields. When methyl cinnamate was used, a mixture of two regioisomers **3ka** and **3ka'** was obtained. Various types of electron-deficient alkenes, such as α,β-unsaturated cyclic ketones, activated indole derivative, vinyl sulfone, and vinyl phosphonate, were also applicable to the present method, affording structurally diverse dialkyl ketones **3la**–**3pa**.

We then turned our attention to the scope of unactivated or electron-rich alkenes **2** as the fragment of 2nd step. Dehydroalanine derivative **1j** was used as a suitable alkene for the 1st step of these reactions, affording α-monosubstituted amino acid derivatives containing various functionalities as the final product. 3-Butenyl benzoate derivatives with a range of substituents at *para* position of the phenyl group provided the corresponding products **3jb**–**3jf** in good yields. Terminal alkenes bearing reactive functional groups, such as hydroxy, (pseudo)halogen, acetyl, silyl, and epoxy groups, were well tolerated (**3jg**–**3jm**). In addition, relatively acidic C–H bond of malonate moiety and N–H bonds of protected amino groups were also successfully incorporated to the products (**3jn**–**3jp**). These examples display the high functional group tolerance of our method. On the other hand, an alkene with basic pyridine moiety showed a decreased reactivity, probably due to the interference with the formation of phosphonium oxalate (**3jr**). Beside monosubstituted alkenes, a cyclic alkene and α,α-disubstituted alkenes were also amenable to this method, furnishing the desired products **3js**–**3jv** in moderate to good yields. The reactions with enol ethers as electron rich alkenes proceeded well to afford the corresponding products **3jw**–**3jx**.

Encouraged by the broad scope of alkenes for both steps, we conducted the radical linchpin coupling with complex alkene fragments derived from biorelevant molecules (Figure 6). The derivatives of naturally occurring bioactive compounds, such as *l*-menthol and deoxycholic acid, and ibuprofen as a representative pharmaceutical were successfully employed for the sequential photocatalysis (**7a**–**7c**). Natural and unnatural amino acids, including *L*-proline, *L*-cysteine, α-allylalanine, and *L*-serine, could be incorporated to afford the desired 1,4-carbonyl products in moderate to high yields (**7d**–**7g**). The same protocol was also applicable to sugar derivatives as the acetonide form (**7h**–**7i**). Finally, two kinds of biorelevant compounds, *L*-serine and vinclozolin, could be connected to furnish the product **7j** in one pot, demonstrating the utility of our method as a tool for rapid connection of two complex molecules.

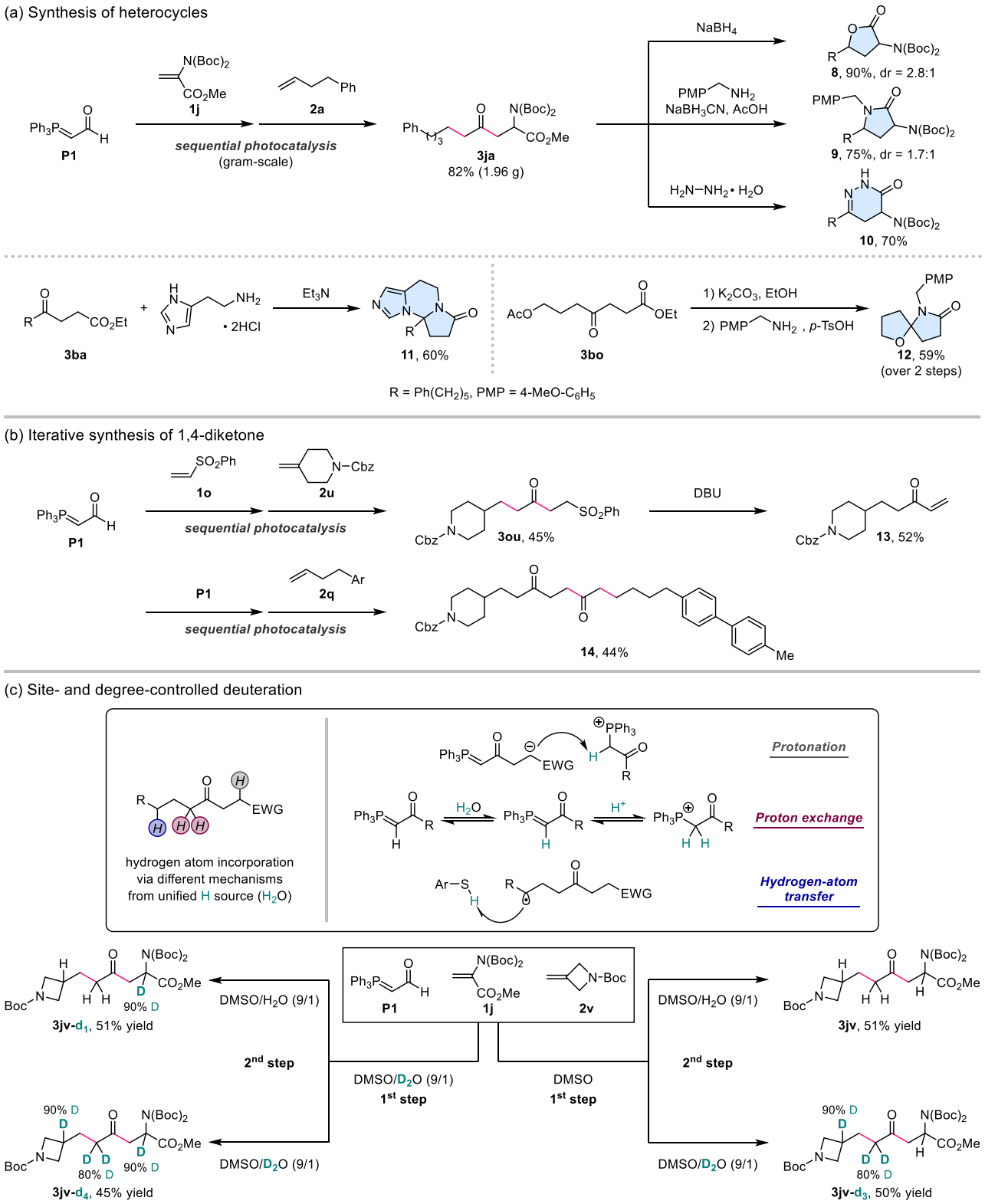

Figure 7. Synthetic applications. See SI for details.

Taking advantage of the utility of products and a characteristic reaction mechanism, several synthetic applications of the sequential photocatalysis were carried out (Figure 7). Firstly, as 1,4-dicarbonyls can be transformed into a diverse array of structures by making use of their two carbonyl moieties, the obtained 1,4-dicarbonyl products were derivatized to access various heterocycles (Figure 7a). As a model product, γ-oxoester **3ja** could be synthesized in a gram scale (see SI for details). Transformations of a ketone moiety of **3ja**, such as reduction, reductive amination, and condensation, gave rise to a new oxygen or nitrogen nucleophile, which subsequently reacted with the terminal ester group to form cyclized products **8**–**10** in good to high yields. The reaction of other γ-oxoester **3ba** with histamine as a bis-

nucleophile produced a fused triazaheterocycle **11**, which is a synthetic congener of glochidine.[23] Furthermore, the deacetylation of a terminal acetoxy group of **3bo**, followed by a tandem imine formation/aminoacetalyzation/amidation sequence, afforded spirocyclic aminoacetal **12** in 2 steps. Next, our protocol was applied to an iterative strategy for synthesis of 1,4-diketone (Figure 7b). The sequential photocatalysis using **P1**, **1o**, and **2u** under the optimal conditions provided the corresponding β-sulfonyl ketone **3ou**, which could be converted to α,β-unsaturated ketone **13** by a base-promoted β-elimination of the sulfonyl group. Repeating the sequential process to assemble **13** with linchpin **P1** and another alkene **2q** successfully proceeded to afford the desired 1,4-diketone **14**. This approach potentially expands the scope of accessible 1,4-dicarbonyl products using our method. Lastly, we sought to synthesize a series of deuterated isotopomers of the product in a site- and degree-controlled manner, which is enabled by the unique mechanism of the present method (Figure 7c). Specifically, three kinds of C–H bonds in the target structure are formed during the sequential process via different mechanisms for incorporation of hydrogen atom: protonation at the α-carbon of ester group, reversible proton exchange at the ylide-derived α-carbon, and hydrogen-atom transfer from thiol catalyst to carbon-centered radical derived from unactivated alkene. Notably, H_2O can serve as a unified hydrogen source for these mechanisms. Therefore, we modified the protocol for sequential process, where a readily available deuterium source D_2O was added or replaced with H_2O at each step according to the desired degree of deuteration of the product. As a result, while non-deuterated product **3jv** was obtained in 51% yield under the optimal conditions using **P1**, **1j**, and **2v**, the use of cosolvent of DMSO and D_2O (v/v = 9/1) only at the 1st step afforded mono-deuterated product **3jv-d$_1$** without affecting the product yield. Moreover, the replacement of H_2O with D_2O at the 2nd step provided tri-deuterated product **3jv-d$_3$**, and the use of DMSO/D_2O cosolvent at both steps furnished tetra-deuterated product **3jv-d$_4$** as a major product. These results demonstrate that our method is useful for preparation of selectively deuterated molecules.[24]

Conclusions

In summary, a sequential photocatalysis involving two mechanistically distinct radical additions has been developed. This process is enabled by multiple roles of ambiphilic radical linchpin **P1**, which serves as a nucleophilic and an electrophilic carbon-centered radical source, as well as a HAT mediator, in the presence of a single photoredox catalyst. A variety of alkene fragments, such as those with reactive functional groups under polar mechanism and biologically relevant complex molecules, can be involved in the bidirectional formations of two C–C bonds from **P1** in one pot. Overall, the present radical linchpin coupling strategy has enabled a rapid and modular access to synthetically valuable 1,4-dicarbonyl compounds. Further investigations on the radical reactivity of phosphonium ylides, especially as a novel HAT catalyst platform, are currently underway in our laboratory.

ASSOCIATED CONTENT

Supporting Information

The Supporting Information is available free of charge at http://pubs.acs.org.

Experimental procedures, mechanistic studies, compound characterization data, and NMR spectra (PDF)

AUTHOR INFORMATION

Corresponding Author

Akira Matsumoto – *Graduate School of Pharmaceutical Sciences, Kyoto University, Sakyo, Kyoto 606-8501, Japan*; orcid.org/0000-0002-3719-8597; Email: matsumoto.akira.3c@kyoto-u.ac.jp

Keiji Maruoka – *Graduate School of Pharmaceutical Sciences, Kyoto University, Sakyo, Kyoto 606-8501, Japan; Guangdong University of Technology, Guangzhou, China*; orcid.org/0000-0002-0044-6411; Email: maruoka.keiji.4w@kyoto-u.ac.jp

Author

Natsumi Maeda – *Graduate School of Pharmaceutical Sciences, Kyoto University, Sakyo, Kyoto 606-8501, Japan*.

Notes

The authors declare no competing financial interest.

ACKNOWLEDGMENT

K.M. gratefully acknowledges financial support via JSPS KAKENHI grant No. 21H05026. A.M. is thankful for financial support via JSPS KAKENHI grant No. 22K14680. The authors thank Kishida chemical Co., Ltd. for donation of (*R*)-*N*-Boc-α-allylalanine ethyl ester (starting material of **7f**).

REFERENCES

(1) (a) Herrera, R. P.; Marqués-López, E. *Multicomponent Reactions: Concepts and Applications for Design and Synthesis*; Wiley: New York, 2015 (b) Zhi, S.; Ma, X.; Zhang, W. Consecutive Multicomponent Reactions for the Synthesis of Complex Molecules. *Org. Biomol. Chem.* **2019**, *17*, 7632–7650. (c) Dömling, A.; Wang, W.; Wang, K. Chemistry and Biology of Multicomponent Reactions. *Chem. Rev.* **2012**, *112*, 3083–3135. (d) Ruijter, E.; Scheffelaar, R.; Orru, R. V. A. Multicomponent Reaction Design in the Quest for Molecular Complexity and Diversity. *Angew. Chem., Int. Ed.* **2011**, *50*, 6234–6246. (e) Touré, B. B.; Hall, D. G. Natural Product Synthesis Using Multicomponent Reaction Strategies. *Chem. Rev.* **2009**, *109*, 4439–4486.

(2) (a) Smith, A. B., III; Boldi, A. M. Multicomponent Linchpin Couplings of Silyl Dithianes via Solvent-Controlled Brook Rearrangement. *J. Am. Chem. Soc.* **1997**, *119*, 6925–6926. (b) Smith, A. B., III; Pitram, S. M.; Boldi, A. M.; Gaunt, M. J.; Sfouggatakis, C.; Moser, W. H. Multicomponent Linchpin Couplings. Reaction of Dithiane Anions with Terminal Epoxides, Epichlorohydrin, and Vinyl Epoxides: Efficient, Rapid, and Stereocontrolled Assembly of Advanced Fragments for Complex Molecule Synthesis. *J. Am. Chem. Soc.* **2003**, *125*, 14435–14445. (c) Nicewicz, D. A.; Johnson, J. S. Three-Component Coupling Reactions of Silylglyoxylates, Alkynes, and Aldehydes: A Chemoselective One-Step Glycolate Aldol Construction. *J. Am. Chem. Soc.* **2005**, *127*, 6170–6171. (d) Heller, S. T.; Newton, J. N.; Fu, T.; Sarpong, R. One-Pot Unsymmetrical Ketone Synthesis Employing a Pyrrole-Bearing Formal Carbonyl Dication Linchpin Reagent. *Angew. Chem., Int. Ed.* **2015**, *54*, 9839–9843. (e) Murray, S. A.; Liang, M. Z.; Meek, S. J. Stereoselective Tandem Bis-Electrophile Couplings of Diborylmethane. *J. Am. Chem. Soc.* **2017**, *139*, 14061–14064. (f) Zhang, L.; Lovinger, G. J.; Edelstein, E. K.; Szymaniak, A. A.; Chierchia, M. P.; Morken, J. P. Catalytic Conjunctive Cross-Coupling Enabled by Metal-Induced Metallate Rearrangement. *Science* **2016**, *351*, 70–74. (g) Hurst, T. E.; Deichert, J. A.; Kapeniak, L.; Lee, R.; Harris, J.; Jessop, P. G.; Snieckus, V. Sodium

Methyl Carbonate as an Effective C1 Synthon. Synthesis of Carboxylic Acids, Benzophenones, and Unsymmetrical Ketones. *Org. Lett.* **2019**, *21*, 3882–3885.

(3) (a) Deng, Y.; Smith, A. B., III. Evolution of Anion Relay Chemistry: Construction of Architecturally Complex Natural Products. *Acc. Chem. Res.* **2020**, *53*, 988–1000. (b) Boyce, G. R.; Greszler, S. N.; Johnson, J. S.; Linghu, X.; Malinowski, J. T.; Nicewicz, D. A.; Satterfield, A. D.; Schmitt, D. C.; Steward, K. M. Silyl Glyoxylates. Conception and Realization of Flexible Conjunctive Reagents for Multicomponent Coupling. *J. Org. Chem.* **2012**, *77*, 4503–4515.

(4) (a) Yan, M.; Lo, J. C.; Edwards, J. T.; Baran, P. S. Radicals: Reactive Intermediates with Translational Potential. *J. Am. Chem. Soc.* **2016**, *138*, 12692–12714. (b) Studer, A.; Curran, D. P. Catalysis of Radical Reactions: A Radical Chemistry Perspective. *Angew. Chem., Int. Ed.* **2016**, *55*, 58–102. (c) Romero, K. J.; Galliher, M. S.; Pratt, D. A.; Stephenson, C. R. J. Radicals in Natural Product Synthesis. *Chem. Soc. Rev.* **2018**, *47*, 7851–7866.

(5) (a) Shaw, M. H.; Twilton, J.; MacMillan, D. W. C. Photoredox Catalysis in Organic Chemistry. *J. Org. Chem.* **2016**, *81*, 6898–6926. (b) Romero, N. A.; Nicewicz, D. A. Organic Photoredox Catalysis. *Chem. Rev.* **2016**, *116*, 10075–10166. (c) McAtee, R. C.; McClain, E. J.; Stephenson, C. R. J. Illuminating Photoredox Catalysis. *Trends Chem.* **2019**, *1*, 111–125.

(6) Novaes, L. F. T.; Liu, J.; Shen, Y.; Lu, L.; Meinhardt, J. M.; Lin, S. Electrocatalysis as an Enabling Technology for Organic Synthesis. *Chem. Soc. Rev.* **2021**, *50*, 7941–8002.

(7) (a) Yang, B.; Lu, S.; Wang, Y.; Zhu, S. Diverse Synthesis of C2-Linked Functionalized Molecules via Molecular Glue Strategy with Acetylene. *Nat. Commun.* **2022**, *13*, 1858. (b) Kim, S.; Yoon, J.-Y. Free Radical-Mediated Ketone Synthesis from Alkyl Iodides via Sequential Radical Acylation Approach. *J. Am. Chem. Soc.* **1997**, *119*, 5982–5983. (c) Anthore-Dalion, L.; Liu, Q.; Zard, S. Z. A Radical Bidirectional Fragment Coupling Route to Unsymmetrical Ketones. *J. Am. Chem. Soc.* **2016**, *138*, 8404–8407.

(8) (a) Trost, B. M.; Hung, C.-I.; Saget, T.; Gnanamani, E. Branched Aldehydes as Linchpins for the Enantioselective and Stereodivergent Synthesis of 1,3-Aminoalcohols Featuring a Quaternary Stereocentre. *Nature Catalysis* **2018**, *1*, 523–530. (b) Hayashi, Y.; Saitoh, T.; Arase, H.; Kawauchi, G.; Takeda, N.; Shimasaki, Y.; Sato, I. Two-Pot Synthesis of Chiral 1,3-*syn*-Diols through Asymmetric Organocatalytic Aldol and Wittig Reactions Followed by Domino Hemiacetal/Oxy-Michael Reactions. *Chem.—Eur. J.* **2018**, *24*, 4909–4915.

(9) Banerjee, A.; Lei, Z.; Ngai, M.-Y. Acyl Radical Chemistry via Visible-Light Photoredox Catalysis. *Synthesis* **2019**, *51*, 303–333.

(10) For recent reviews on photoinduced Hydrogen-atom transfer: (a) Cao, H.; Tang, X.; Tang, H.; Yuan, Y.; Wu, J. Photoinduced Intermolecular Hydrogen Atom Transfer Reactions in Organic Synthesis. *Chem. Catalysis* **2021**, *1*, 523–598. (b) Capaldo, L.; Ravelli, D.; Fagnoni, M. Direct Photocatalyzed Hydrogen Atom Transfer (HAT) for Aliphatic C−H Bonds Elaboration. *Chem. Rev.* **2022**, *122*, 1875–1924. (c) Capaldo, L.; Quadri, L. L.; Ravelli, D. Photocatalytic Hydrogen Atom Transfer: The Philosopher's Stone for Late-Stage Functionalization? *Green Chem.* **2020**, *22*, 3376–3396.

(11) (a) Lenardon, G. V. A.; Nicchio, L.; Fagnoni, M. Photogenerated Electrophilic Radicals for the Umpolung of Enolate Chemistry. *J. Photochem. Photobiol. C* **2021**, *46*, 100387. (b) Lee, K. N.; Ngai, M. Y. Recent Developments in Transition-Metal Photoredox-Catalysed Reactions of Carbonyl Derivatives. *Chem. Commun.* **2017**, *53*, 13093–13112.

(12) Mečiarová, M.; Tisovský, P.; Šebesta, R. Enantioselective Organocatalysis Using SOMO Activation. *New J. Chem.* **2016**, *40*, 4855–4864.

(13) Lemmerer, M.; Schupp, M.; Kaiser, D.; Maulide, N. Synthetic Approaches to 1,4-Dicarbonyl Compounds. *Nat. Synth.* **2022**, *1*, 923–935.

(14) Rohe, S.; Morris, A. O.; McCallum, T.; Barriault, L. Hydrogen Atom Transfer Reactions via Photoredox Catalyzed Chlorine Atom Generation. *Angew. Chem., Int. Ed.* **2018**, *57*, 15664–15669.

(15) Miura, T.; Funakoshi, Y.; Nakahashi, J.; Moriyama, D.; Murakami, M. Synthesis of Elongated Esters from Alkenes. *Angew. Chem., Int. Ed.* **2018**, *57*, 15455–15459.

(16) Lamy, E.; Nadjo, L.; Saveant, J. M. Standard Potential and Kinetic Parameters of the Electrochemical Reduction of Carbon Dioxide in Dimethylformamide. *J. Electroanal. Chem.* **1977**, *78*, 403–407.

(17) For selected examples: (a) Huang, Y.; Hou, J.; Zhan, L.-W.; Zhang, Q.; Tang, W.-Y.; Li, B.-D. Photoredox Activation of Formate Salts: Hydrocarboxylation of Alkenes via Carboxyl Group Transfer. *ACS Catal.* **2021**, *11*, 15004–15012. (b) Alektiar, S. N.; Wickens, Z. K. Photoinduced Hydrocarboxylation via Thiol-Catalyzed Delivery of Formate Across Activated Alkenes. *J. Am. Chem. Soc.* **2021**, *143*, 13022–13028. (c) Chmiel, A. F.; Williams, O. P.; Chernowsky, C. P.; Yeung, C. S.; Wickens, Z. K. Non-Innocent Radical Ion Intermediates in Photoredox Catalysis: Parallel Reduction Modes Enable Coupling of Diverse Aryl Chlorides. *J. Am. Chem. Soc.* **2021**, *143*, 10882–10889. (d) Hendy, C. M.; Smith, G. C.; Xu, Z.; Lian, T.; Jui, N. T. Radical Chain Reduction via Carbon Dioxide Radical Anion ($CO_2^{\bullet-}$). *J. Am. Chem. Soc.* **2021**, *143*, 8987–8992. (e) Wang, H.; Gao, Y.; Zhou, C.; Li, G. Visible-Light-Driven Reductive Carboarylation of Styrenes with CO_2 and Aryl Halides. *J. Am. Chem. Soc.* **2020**, *142*, 8122–8129.

(18) Luo, J.; Zhang, J. Donor–Acceptor Fluorophores for Visible-Light-Promoted Organic Synthesis: Photoredox/Ni Dual Catalytic $C(sp^3)$–$C(sp^2)$ Cross-Coupling. *ACS Catal.* **2016**, *6*, 873–877.

(19) Wan, Y.; Zhu, J.; Yuan, Q.; Wang, W.; Zhang, Y. Synthesis of β-Silyl α-Amino Acids via Visible-Light-Mediated Hydrosilylation. *Org. Lett.* **2021**, *23*, 1406–1410.

(20) (a) Dong, J.-Y.; Xu, W.-T.; Yue, F.-Y.; Song, H.-J.; Liu, Y.-X.; Wang, Q.-M. Visible-Light-Mediated Deuteration of Aldehydes with D_2O via Polarity-Matched Reversible Hydrogen Atom Transfer. *Tetrahedron* **2021**, *82*, 131946. (b) Zhang, Y.; Ji, P.; Dong, Y.; Wei, Y.; Wang, W. Deuteration of Formyl Groups via a Catalytic Radical H/D Exchange Approach. *ACS Catal.* **2020**, *10*, 2226–2230.

(21) Draper, F.; Doeven, E. H.; Adcock, J. L.; Francis, P. S.; Connell, T. U. Extending Photocatalyst Activity through Choice of Electron Donor. *J. Org. Chem.* **2023**. https://doi.org/10.1021/acs.joc.2c02460.

(22) Ruffoni, A.; Mykura, R. C.; Bietti, M.; Leonori, D. The Interplay of Polar Effects in Controlling the Selectivity of Radical Reactions. *Nature Synthesis* **2022**, 1, 682–695.

(23) Seo, J. M.; Hassan, A. H. E.; Lee, Y. S. An Expeditious Entry to Rare Tetrahydroimidazo[1,5-*c*]pyrrolo[1,2-*a*]pyrimidin-7(8*H*)-ones: A Single-Step Gateway Synthesis of Glochidine Congeners. *Tetrahedron* **2019**, *75*, 130760.

(24) Zhou, X.; Yu, T.; Dong, G. Site-Specific and Degree-Controlled Alkyl Deuteration via Cu-Catalyzed Redox-Neutral Deacylation. *J. Am. Chem. Soc.* **2022**, *144*, 9570–9575.

Insert Table of Contents artwork here